

Numerical analysis of the effective masses in InGaAsN quantum-well structures with self-consistent effects

This article has been downloaded from IOPscience. Please scroll down to see the full text article.

2005 J. Phys.: Condens. Matter 17 6539

(<http://iopscience.iop.org/0953-8984/17/41/023>)

View [the table of contents for this issue](#), or go to the [journal homepage](#) for more

Download details:

IP Address: 129.252.86.83

The article was downloaded on 28/05/2010 at 06:10

Please note that [terms and conditions apply](#).

Numerical analysis of the effective masses in InGaAsN quantum-well structures with self-consistent effects

M S Wartak and P Weetman

Department of Physics and Computer Science, Wilfrid Laurier University, Waterloo, ON, N2L 3C5, Canada

Received 12 July 2005, in final form 5 September 2005

Published 30 September 2005

Online at stacks.iop.org/JPhysCM/17/6539

Abstract

A systematic analysis of the electrostatic effects on the effective masses of holes in $\text{In}_y\text{Ga}_{1-y}\text{As}_{1-x}\text{N}_x/\text{GaAs}$ quantum-well structures was performed. A 10-band $k \cdot p$ Hamiltonian matrix was used in the calculations and solved self-consistently with the Poisson equation. Numerical results have been presented for a large range of material and structural parameters. Our results show that significant variation in the effective masses is possible by adjusting the relevant parameters and that the effects due to self-consistency are small for most subbands.

1. Introduction

Semiconductor lasers based on quantum wells [1] have found important applications in fibre-optics communication systems, in biophotonics, in optical sensing, and in several other areas. Their design and fabrication is a costly and time-consuming process. A significant role in the design and simulation process is played by the reliable knowledge of fundamental parameters. One such parameter is the effective mass of holes. For the $\text{In}_{1-x}\text{Ga}_x\text{As}/\text{InGaAsP}$ material system we have carried out a systematic numerical analysis of that parameter for a large range of material parameters and quantum-well widths [2].

In recent years significant progress in the research on a new class of material based on nitride semiconductors [3] had been advanced. It has been found that replacing a small amount of the group V element by nitrogen in a III–V material system reduces the energy gap. This reduction significantly changes the band structure and offers new possibilities of improving the optoelectronic properties of devices based on those materials.

In the present paper we report on the numerical work aimed at determining effective masses of holes in $\text{In}_{1-x}\text{Ga}_x\text{As}_{1-y}\text{N}_y$ which were determined for a wide range of N compositions and well widths. We have also performed an analysis of the effects of self-consistency, which consists in a self-consistent solution of the matrix Schrödinger equation and the Poisson equation.

In section 2 we outline our formalism and in section 3 we present and discuss our results.

2. Formalism

We based our approach on the method presented by Tomić *et al* [4], where the effect of adding N to the structure is modelled perturbatively because the $\text{In}_{1-x}\text{Ga}_x\text{As}_{1-y}\text{N}_y$ layers have small values of y . An 8×8 Luttinger–Kohn (LK) method (coupled model of conduction, heavy, light, and split-off hole bands) is used with the $\text{In}_{1-x}\text{Ga}_x\text{As}_{1-y}\text{N}_y$ layers replaced by $\text{In}_{1-x}\text{Ga}_x\text{As}$ (known as the host structure). When a small amount of N is introduced, the 8×8 Hamiltonian is expanded to a 10×10 Hamiltonian to account for coupling to the ‘nitrogen band’ (given by the first and sixth rows and columns in the Hamiltonian below). Additionally some of the terms from the 8×8 contribution are modified due to the inclusion of N. The resulting 10×10 Hamiltonian is

$$H = \begin{pmatrix} E_N & V_{\text{Nc}} & 0 & 0 & 0 & 0 & 0 & 0 & 0 & 0 \\ & E_C & -\sqrt{3}T_+ & \sqrt{2}U & -U & 0 & 0 & 0 & -T_- & -\sqrt{2}T_- \\ & & E_{\text{HH}} & \sqrt{2}S & -S & 0 & 0 & 0 & -R & -\sqrt{2}R \\ & & & E_{\text{LH}} & Q & 0 & T_+^* & R & 0 & \sqrt{3}S \\ & & & & E_{\text{SO}} & 0 & \sqrt{2}T_+^* & \sqrt{2}R & -\sqrt{3}S & 0 \\ & & & & & E_N & V_{\text{Nc}} & 0 & 0 & 0 \\ & & & & & & E_C & -\sqrt{3}T_- & \sqrt{2}U & -U \\ & & & & & & & E_{\text{HH}} & \sqrt{2}S^* & -S^* \\ & & & & & & & & E_{\text{LH}} & Q \\ & & & & & & & & & E_{\text{SO}} \end{pmatrix} \quad (1)$$

where the subscripts N, C, HH, LH, and SO stand for nitrogen, conduction, heavy-hole, light-hole, and split-off bands, respectively. We do not show the lower triangle as this matrix is Hermitian. The diagonal terms of the 8×8 component of this Hamiltonian are [1, 4]

$$\begin{aligned} E_C &= E_{C0} + \frac{\hbar^2}{2m_0} s_c (k_{\parallel}^2 + k_z^2) - (\alpha - \kappa)y \\ E_{\text{HH}} &= E_{\text{HH0}} - \frac{\hbar^2}{2m_0} ((\gamma_1 + \gamma_2)k_{\parallel}^2 + (\gamma_1 - 2\gamma_2)k_z^2) + \kappa y \\ E_{\text{LH}} &= E_{\text{LH0}} - \frac{\hbar^2}{2m_0} ((\gamma_1 - \gamma_2)k_{\parallel}^2 + (\gamma_1 + 2\gamma_2)k_z^2) + \kappa y \\ E_{\text{SO}} &= E_{\text{SO0}} - \frac{\hbar^2}{2m_0} \gamma_1 (k_{\parallel}^2 + k_z^2) + \kappa y. \end{aligned}$$

Here the first terms on the RHS of these equations represent the band-edge energies of the host system, which are found using a band-offset model that incorporates strain [1, 4]. The last terms on the RHS of these equations represent the modification due to the N band; y is the fraction of N in the structure, α and κ are parameters which are chosen to be 1.75 and 3.5, respectively [4]. The term $s_c = 1/m_c^* - (E_P/3)[2/E_g + 1/(E_g + \Delta_{\text{SO}})]$ is used in place of $1/m_c^*$ and the Luttinger coefficients are replaced by $\gamma_1 \rightarrow \gamma_1 - E_P/(3E_g^{\text{h}})$, $\gamma_{2,3} \rightarrow \gamma_{2,3} - E_P/(6E_g^{\text{h}})$ in the 8×8 model (E_P and E_g^{h} are the optical matrix parameter and bandgap of the host material, respectively). The other 8×8 terms are standard [1]:

$$\begin{aligned} T_{\pm} &= \frac{1}{\sqrt{6}} P(k_x \pm ik_y) \\ U &= \frac{1}{\sqrt{3}} Pk_z \\ S &= \sqrt{\frac{3}{2}} \frac{\hbar^2}{m_0} \gamma_3 k_z (k_x - ik_y) \end{aligned}$$

$$R = \frac{\sqrt{3}}{2} \frac{\hbar^2}{2m_0} [(\gamma_2 + \gamma_3)(k_x - ik_y)^2 - (\gamma_3 - \gamma_2)(k_x + ik_y)^2]$$

$$Q = -\frac{\hbar^2}{m_0} \left(\frac{1}{\sqrt{2}} \gamma_2 k_{\parallel}^2 - \sqrt{2} \gamma_2 k_z^2 \right) - \sqrt{2} \eta_{ax}$$

with P being the Kane matrix element for the conduction band and the last term in the expression for Q being the shear strain component [1, 4]. The N band components of the Hamiltonian are

$$E_N = E_{N0} + \delta E_N^{hy} - (\gamma - \kappa)y \quad (2)$$

where E_{N0} is the band-edge of the N band, including strain (which is just the hydrostatic component). Table III of Choulis *et al* [5] gives material data for the InN and GaN systems. The difference between the unstrained conduction and N energy bands of 0.485 eV has been taken from Tomić *et al* [4]. V_{Nc} is the only N band coupling term. It describes the interaction between the N and C bands and is given by

$$V_{Nc} = -\beta\sqrt{y}. \quad (3)$$

Values for γ and β are 3.5 and 1.675, respectively [4].

The effective masses were found by a least-squares fitting of a parabolic energy dispersion curve to the actual dispersion curve calculated from the 10×10 method. We took the $k = 0$ energies found from the 10×10 model as the $k = 0$ energies of a parabolic model

$$E_{n,\text{parab}}(k) = E_{n,10 \times 10}(0) + \frac{\hbar^2}{2m_n^*} k^2 \quad (4)$$

where n denotes the n th hole band. The fitting parameter is then the band's effective mass m_n^* .

The self-consistent method is similar to the one which we used before [6], which consists in a self-consistent solution of the Poisson's equation with the matrix Schrödinger equation described by Hamiltonian (1). The Poisson equation is

$$\frac{d}{dz} \left[\varepsilon(z) \frac{d}{dz} \phi(z) \right] = -e [\rho_{\text{HH}}(z) + \rho_{\text{LH}}(z) - \rho_{\text{C}}(z)] \quad (5)$$

where e is the fundamental charge, $\varepsilon(z)$ is the position-dependent permittivity, and $\rho_{\text{C}}(z)$, $\rho_{\text{HH}}(z)$ and $\rho_{\text{LH}}(z)$ are the position-dependent electron and hole band density distributions, respectively. The function $\phi(z)$ is the electrostatic potential. The density distributions are [6]

$$\rho_{\alpha}(z) = \frac{k_{\text{B}}T}{\pi \hbar^2} \left\{ \sum_n \bar{m}_{\alpha}^* |F_n^{\alpha}(z)|^2 \ln \left[1 + \exp \left(\frac{E_{\alpha}^{\text{f}} - E_n^{\alpha}}{k_{\text{B}}T} \right) \right] \right\}. \quad (6)$$

The symbol α represents the conduction (C), heavy-hole (HH) and light-hole (LH) bands and n is an index over the subbands. E_{C}^{f} is the conduction band Fermi level and $E_{\text{HH}}^{\text{f}} = E_{\text{LH}}^{\text{f}}$ is the valence band Fermi level. Their values are determined by the standard methods [1]. The symbol k_{B} is Boltzmann's constant, T is temperature, \bar{m}_{α}^* is the average effective mass for the particular band which is approximated as the effective mass in the well since most of the carriers are confined there. $F_n^{\alpha}(z)$ and E_n^{α} are the respective envelope eigenfunctions and eigenvalues of the various subbands in the parabolic approximation at the band-edge.

3. Results and discussion

Our analysis was performed for undoped $\text{In}_{0.36}\text{Ga}_{0.64}\text{As}_{1-y}\text{N}_y/\text{GaAs}$ systems similar to the one studied by Tomić *et al* [4]. The nitrogen composition (y) changes in the range $0.00 \leq y \leq 0.05$.

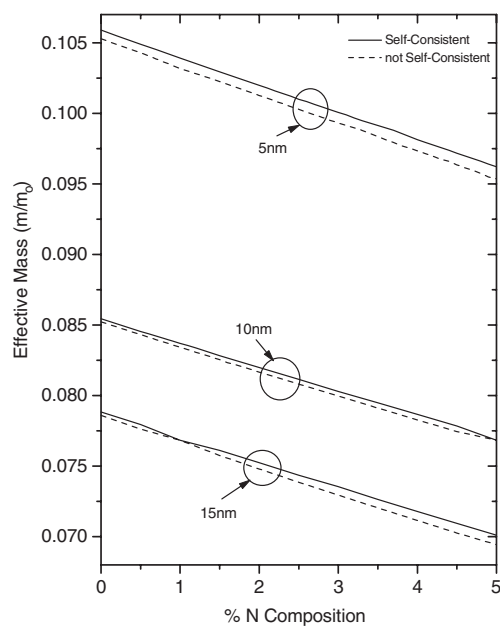


Figure 1. Effective masses of the first band (HH1) versus nitrogen composition in $\text{In}_{0.36}\text{Ga}_{0.64}\text{As}_{1-y}\text{N}_y$ for three well widths with and without self-consistency effects.

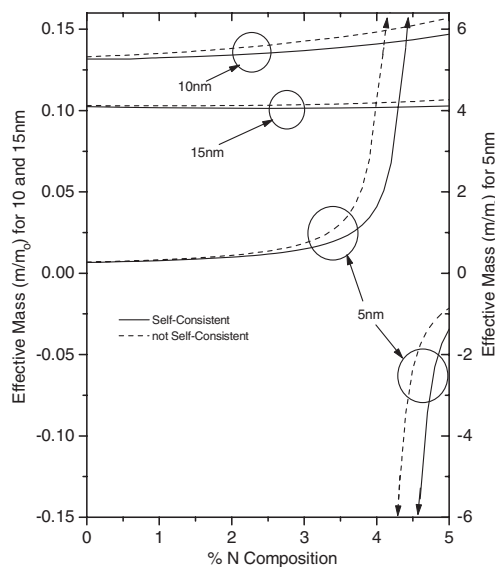


Figure 2. Effective masses of the second band (HH2) versus nitrogen composition in $\text{In}_{0.36}\text{Ga}_{0.64}\text{As}_{1-y}\text{N}_y$ for three well widths with and without self-consistency effects.

The values of well widths considered were 5, 10 and 15 nm. Physical parameters were taken from table III of [5] and we used model-solid theory to calculate band-offsets [1]. The well is strained by the lattice mismatch between it and the GaAs cladding and substrate. The material in the well is designed to operate in the $1.3 \mu\text{m}$ range when the nitrogen is added. We use symmetric boundary conditions [1] and present results for the [100] growth direction.

The results for hole bands are presented in figures 1–5. The calculations were performed with and without electrostatic self-consistency assuming an average carrier density of $10 \times 10^{18} \text{ cm}^{-3}$ in the well. We first discuss the characteristics of the calculations not incorporating self-consistency as the self-consistent results are qualitatively the same.

The effective mass results are shown in figures 1–4. The bands are ordered as HH1 (first heavy-hole), HH2 (second heavy-hole), LH1 (first light-hole) and HH3 (third heavy-hole) as expected for a system under biaxial compression. All figures show a significant difference in the effective masses depending on the well width because the band structure is highly dependent on this quantity. We observe that for the first heavy-hole band the variation of effective mass is less than ten per cent over the nitrogen composition range. Polimeni *et al* [7] mention that band's effective mass will have a small variation against nitrogen composition. Also, our values are close to their estimated values (figure 3 [7]).

Of the three well widths chosen, the 5 nm width is the most affected by the nitrogen composition. In the second and fourth band we see that the effective mass varies significantly in certain regions, going from positive to negative. Consider, for example, figure 2 for the 5 nm well width around 4% nitrogen composition. The band curvature changes from positive to zero to negative. Since the effective mass is proportional to the inverse of band curvature, the relatively small curvature change causes the large changes observed in the effective mass.

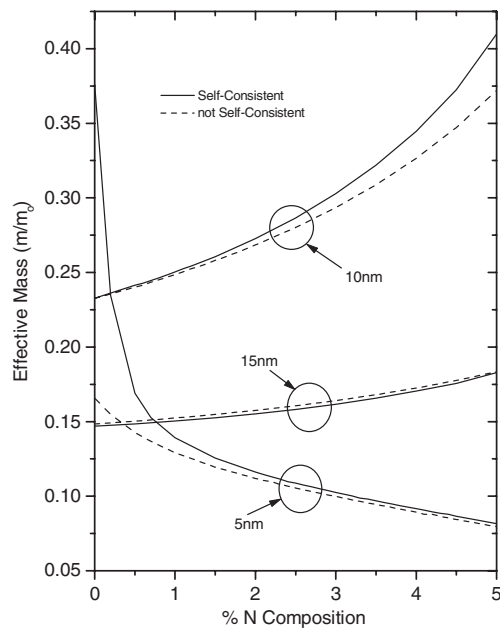


Figure 3. Effective masses of the third band (LH1) versus nitrogen composition in $\text{In}_{0.36}\text{Ga}_{0.64}\text{As}_{1-y}\text{N}_y$ for three well widths with and without self-consistency effects.

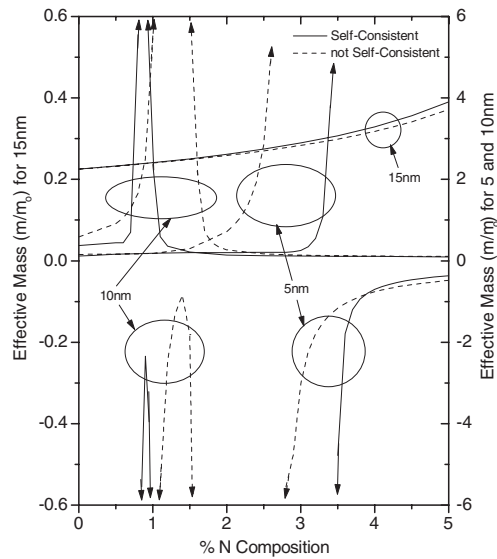


Figure 4. Effective masses of the fourth band (HH3) versus nitrogen composition in $\text{In}_{0.36}\text{Ga}_{0.64}\text{As}_{1-y}\text{N}_y$ for three well widths with and without self-consistency effects.

In figure 5, for the 5 nm well width at 3% nitrogen composition, we show the band dispersions using the 10×10 LK calculations and using a parabolic model utilizing the calculated band-edge effective mass values. We observe that the effective mass dispersions vary significantly from the 10×10 dispersions away from the band-edge as is expected (else a LK approximation would not be necessary). This figure also shows that, in this case, the fourth band has a negative curvature near the band-edge.

We have chosen a rather large carrier concentration to highlight the self-consistency effects on the effective mass. Below a carrier density of around $5 \times 10^{18} \text{ cm}^{-3}$, the effects are not very significant. Quantitatively, the narrower the well, the more significant self-consistency is because narrower wells result in higher energy states. These higher energy states are closer to the barrier energies where the heterostructure potential is modified the most by electrostatics. Self-consistency has the largest effect near a sign transition of the effective mass (see for example figure 4) because this is near zero band-curvature. Small changes in potential and hence curvature will correspond to large changes in effective mass in those regions.

4. Conclusions

Hole effective masses were calculated numerically for a range of material compositions and quantum-well widths. Results showed that by adjusting the composition and/or well width, effective masses can be effectively modified. By controlling their values, one can design specific structures for specific device requirements.

Additionally, the effects of electrostatic self-consistency on the effective mass were analysed. In general, self-consistency does not change the effective mass significantly. It

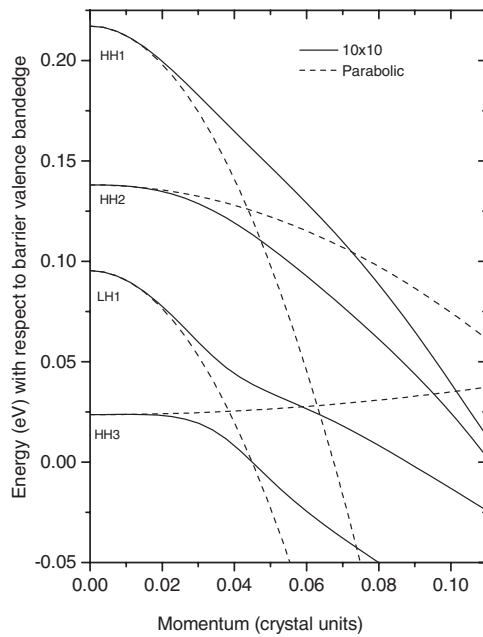


Figure 5. Band dispersions using the 10×10 calculations and a parabolic model with the calculated effective masses. The results are for the non-self-consistent calculation of the 5 nm well width at 3% nitrogen composition.

was found to be the largest around nitrogen composition regions where the effective mass changed signs.

Acknowledgments

We would like to acknowledge the support from the Natural Science and Engineering Research Council of Canada (NSERC) and Sharcnet, Ontario, Canada.

References

- [1] Chuang S L 1995 *Physics of Optoelectronic Devices* (New York: Wiley)
- [2] Ma T A and Wartak M S 1994 *Phys. Rev. B* **50** 15401
- [3] Morkoc H 1999 *Nitride Semiconductor and Devices* (Berlin: Springer)
- [4] Tomić S, O'Reilly E P, Fehse R, Sweeney S J, Adams A R, Andreev A D, Choulis S A, Hosea T J C and Reichert H 2003 *IEEE J. Sel. Top. Quantum Electron.* **9** 1228
- [5] Choulis S A, Hosea T J C, Tomić S, Kamal-Saadi M, Adams A R, O'Reilly E P, Weinstein B A and Klar P J 2002 *Phys. Rev. B* **66** 165321
- [6] Wartak M S, Weetman P, Alajoki T, Aikio J and Heikkinen V 2002 *Microw. Opt. Technol. Lett.* **35** 55
- [7] Polimeni A, Masia F, Vinattieri A, Baldassarri G, von Högersthal H and Capizzi M 2004 *Appl. Phys. Lett.* **84** 2295